LAWRENCE
LIVERMORE
NATIONAL
LABORATORY

LLNL-PROC-432805

Toroidally resolved structure of heat flux in RMP H-mode discharges on DIII-D

M. W. Jakubowski, T. E. Evans, M. E. Fenstermacher, C. J. Lasnier, O. Schmitz, R. C. Wolf, L. B. Baylor, J. A. Boedo, K. H. Burrell, J. S. deGrassie, P. Gohil, R. Laengner, A. W. Leonard, R. A. Moyer, T. W. Petrie, C. C. Petty, R. I. Pinsker, T. L. Rhodes, M. J. Schaffer, P. B. Snyder, H. Stoschus, T. Osborne, D. Orlov, E. Unterberg, J. G. Watkins

May 20, 2010

19th PSI conference
San Diego, CA, United States
May 24, 2010 through May 28, 2010

Disclaimer

Toroidally resolved structure of heat flux in RMP H-mode discharges on DIII-D[†]

M.W. Jakubowski[1], T.E. Evans[3], M.E. Fenstermacher[4], C.J. Lasnier[4], O. Schmitz[2], R.C. Wolf[1], L.B. Baylor[3], J.A. Boedo[5], K.H. Burrell[3], J.S. deGrassie[3], P. Gohil[3], R. Laengner[2], A.W. Leonard[3], R.A. Moyer[5], T.W. Petrie[3], C.C. Petty[3], R.I. Pinsker[3], T.L. Rhodes[5], M.J. Schaffer[3], P.B. Snyder[3], H. Stoschus[2], T. Osborne[3], D. Orlov[5], E. Unterberg[3], J.G. Watkins[6]

[1] Max-Planck-Institut für Plasmaphysik, IPP-EURATOM Association, Greifswald, Germany

[2] Forschungszentrum Jülich, IEF-4, Association FZJ-EURATOM, TEC, Jülich, Germany

[3] General Atomics, P.O. Box 85608, San Diego, California, 92186-5608 U.S.A.

[4] Lawrence Livermore National Laboratory, P.O. Box 808, Livermore, CA 94550, U.S.A.

[5] University of California, San Diego, La Jolla, CA 92093, U.S.A.

[6] Sandia National Laboratory, Albuquerque, New Mexico, U.S.A.

Abstract

An undesirable consequence of this high confinement is the periodic formation of large transient power loads to the plasma facing components due to type-I ELMs. As shown on DIII-D they can be either completely eliminated or mitigated with resonant magnetic perturbation fields. Application of RMP results in a 3D magnetic topology that affects heat loads in ELM-suppressed discharges as well as the smaller ELMs seen during mitigated scenarios. Two infra-red cameras, separated 70 degrees toroidally, were used to make simultaneous measurements of heat loads with high framing rate of type-I ELMs and how they are affected by stochastic boundary. Without the RMP fields ELMs display a variety of different heat load dynamics as measured by two cameras as well as range of toroidal variability in the deposited energy that is characteristic of their 3D structure. On

[†]Work supported in part by the US Department of Energy under DE-FC02-04ER54698, DE-AC52-07NA27344 (LLNL), DE-AC05-00OR22725, DE-AC04-94AL85000, and DE-FG02-07ER54917

average there is no asymmetry between two toroidal locations. With RMP mitigated ELMS, the variability in the power loads is significantly reduced even though asymmetries in power loads are introduced. The scenario when only very small ELMs persist has been achieved. As expected the effect of magnetic perturbations on ELM dynamics depends shows rather resonant character with the optimum of ELM mitigation being reached at q_{95}=3.9 with P_{tot} = 9 MW.

Introduction

It is assumed, that the next step fusion devices, such as ITER, will operate in regimes with high confinement of energy in order to demonstrate good rate of fusion power production. The discharge scenario, which fulfils those requirements, is so-called H-mode [1]. An undesirable consequence of the high confinement is periodic formation of large transient power loads to the plasma facing components due to type-I ELM events [2,3]. In recent years, clear evidence of the ELM as a filamentary structure [4,5] propagating radially across the scrape-off layer (SOL) and extending far outside the separatrix have been shown [6,7]. They also form characteristic patterns on the divertor surface, where several discrete substructures have been measured on ASDEX Upgrade [8] and recently also on DIII-D [9]. The power loads due to type-I ELMs are of great concern for lifetime and durability of the divertors in future devices like ITER [10]. Therefore, there extensive studies of the heat distribution on the plasma facing components are performed in tokamaks. Typically it is assumed, that there is toroidal symmetry of heat loads and the structure of strike lines [3,11] on the divertor surface. On the other hand they are also recent studies [12], which suggest that thermo-electric currents flowing within the filaments form rather three dimensional structures of ELM deposition patterns.

As shown on DIII-D type-I ELMs can be either completely eliminated [13,14] or mitigated with Resonant Magnetic Perturbation (RMP) fields, which stochastically open edge field lines

to the divertor [15,16]. This is a very promising scenario for ITER, as it enhances significantly durability of the material of plasma facing components.

In this work we study in how far the assumption of toroidal symmetry of ELM heat loads to the divertor is valid on DIII-D and how this is affected by application of the magnetic perturbations. It was possible to achieve a regime were very small regular ELMs appear with deposition patterns following manifolds of stochastic boundary. The amplitude and toroidal distribution of heat loads in this regime is sensitive to q_{95}.

Experimental set-up

Previous studies have been performed with ITER-similar shape and with ITER-like electron pedestal collisionality [9]. That configuration was unfavourable for the observation of the outer leg, which was partially covered by the pump duct. Therefore, in this work, plasma has been optimized for the infra-red systems, i.e. outer leg has been pulled out from the pump duct on top of the pump duct shelf (see Figure 1), which resulted in average plasma triangularity about 0.3 and electron pedestal collisionality of $\nu^* \approx 1$. Few important plasma parameters have been presented in Figure 2. The analysis is based on four discharges with all parameters identical but q_{95}, which was varied from 3.5 to 4.3, in order to scan resonant window of interaction between RMPs and plasma magnetic equilibrium. Heat flux density was measured with two infra-red cameras separated toroidally by 70 degrees. At 65 degrees FLIR SC6000 camera with spatial resolution of about 6-7 mm and temporal resolution of 12 kHz and SBF-125 camera with spatial resolution of 9-10 mm and temporal resolution of 13 kHz. Both cameras observed lower divertor floor through a similar optical elements. Absolute calibration of both IR systems was performed during the same machine bake in order to assure similar calibration curves. The heat fluxes on the target surfaces are calculated by applying a standard numerical solution of the two-dimensional heat diffusion equations to the evolution of the surface temperature on the investigated area with the THEODOR code [17].

The code, which is used to study heat loads due to type-I ELMs has the ability to evaluate the influence of the surface layers on the evaluated heat flux density. THEODOR starts from the temporal evolution of the surface temperature distribution along the poloidal target coordinate and computes the heat flux distribution using a 2D slab geometry approximation for the target tiles, introducing the real poloidal target width and an averaged target thickness. Front surface layers are taken into account with the heat transmission coefficient α, which is chosen in such a way that negative heat fluxes in the inter-ELM period are avoided. . The coefficient assumes the same surface properties across the strike line, which is not necessarily correct; therefore, some caution must be taken with absolute numbers of the heat flux density. A detailed discussion of the method on examples of ASDEX-Upgrade and JET data is given in [17,18]. In this work choice of α coefficient was rather critical as we perform comparison of both camera data at two different toroidal locations. One of the main criterions is how the heat flux behaves in the decay phase. We have assumed following [17,18] that negative values would be unphysical. We have set α always to highest possible value possible, that power flux q [MW] did not become negative. Typical values for inner leg are 100 [$kWm^{-2}K^{-1}$] at 65 degrees and 40 [$kWm^{-2}K^{-1}$] at 135 degrees and 65 – 70 [$kWm^{-2}K^{-1}$] for the outer leg at both locations. As the evaluated time behaviour of heat flux density at the strike point during an ELM is much more sensitive to the choice of α then integrated over time energy we have decided to calculate toroidal asymmetries during ELMs from energy stored during an ELM rather than heat flux density.

Investigated discharges had been divided into four different phases (see Figure 2)

1. Initial RMP phase ($t < 1500$ ms), where we have tried to see in how far can one control ELMs with magnetic perturbation turned on before onset of the H-mode.
2. No RMP phase (1500 ms $< t < 2200$ ms) with very low level of I-coil current (below 1 kA) as a reference case for the time with RMP turned on

3. RMP and 6 MW of total heating power (2200 ms < t 3000 ms). To study the influence of stochastic boundary on ELMs with magnetic perturbation applied during an H-mode.
4. RMP and 9 MW of total heating power (t > 3000 ms) . Higher heating power was established to study beta effects on penetration of magnetic perturbation field.

Experimental results

An example of results for one of the investigated discharges (#139745, q_{95} = 3.9) is shown in. There is little or almost no effect of I-coil currents on behaviour of ELMs in the in the initial phase (t < 1500 ms), which suggests rather weak interaction between RMP and the plasma. Although we observe larger ELMs in the second phase, when RMP has been switched off, it is rather an effect of increased heating power. Switching on magnetic perturbations at t = 2200 ms reduces amplitudes of ELMs by roughly 30%. As it will be shown later how the ELMs are affected by RMP strongly depends on the value of q_{95}. Increasing heating power to 9 MW at t = 3000 ms reduces ELMs even stronger; they amplitude is reduced by almost factor of 3 as compared to non-RMP phase. This is rather robust effect for all discharges, higher heating power results in better coupling of magnetic perturbation with plasma magnetic equilibrium. This seems to be in contradiction to present theories on penetration of external fields [19]. One would expect that higher plasma rotation and pedestal temperature should help screen penetration more effectively.

In Figure 3 several parameters characterizing ELMs in different stages of the discharge are presented. Quantities presented there are averaged over all events in given phase with error bars equal to standard deviation. This gives an estimate of variability for a given parameter. From top to bottom three different parameters are shown as a function of q95 (the abscissa): mean energy deposited to the lower divertor (sum of inner and outer leg) averaged over both

toroidal locations (*E* [kJ]), increase rate of wetted area with ELM energy (*A* [m/J]) and toroidal asymmetry between deposited energy measured at two toroidal locations (*R*). Blue squares show results for non-RMP phase, red triangles for the time range (2300 < t < 3000 ms) with RMP and 6 MW of total heating power and green diamonds for the phase with RMP and 9 MW of heating power (3500 < t < 4200).

The average energy in no-RMP phase changes with q95 from slightly above 8 kJ at q_{95} = 3.5 to 7 kJ at q_{95}=4.3 with standard deviation of order of 50%. Introducing RMP can significantly reduce average size of ELM as well as variability of the deposited energy. Red curve shows reduction of *E* to 5 kJ with standard deviation of about 1 kJ; as the q95 increases the level of reduction is smaller. From q95 > 4.1 *E* has the same value as without magnetic perturbation. Nevertheless, variability remains smaller for all the investigated cases. Introducing higher heating power (green curve) makes ELMs lesser as compared to 6 MW case. There is no data point for q_{95} = 3.5 as increasing the neutral beam injection triggered a tearing mode. At higher power we see similar tendency, approaching with q_{95} to the value of 3.5 decreases average ELM size to about 3 kJ at q_{95} = 3.9. The variability of the ELM size is smaller than in the non-RMP case as well as in the case with RMP and P_{tot} = 6 MW.

Middle graph in Figure 3 shows how the wetted area changes with the ELM size. It was already shown in [9], that during an H-mode discharge wetted area of type-I ELM on the divertor surface is a linear function of ELM size (expressed as an amount of energy expelled from plasma during an event). Also it was shown there, that introducing proper level of magnetic perturbation makes wetted area independent on the ELM size. In order to see in how far effect of magnetic perturbation on ELM control depends on q_{95} we introduce parameter *A,* which is simply a value of slope in linear polynomial fit of a function $w = f(E_{dep})$, where *w* is the wetted area and E_{dep} is energy deposited to the divertor. Without RMP (see blue curve in Figure 3) *A* is a linear function of q95, i.e. wetted area increases faster with ELM size at

higher q_{95} (lower plasma current), which suggests that at higher plasma current ELMs with the same energy propagate radial outwards with higher velocity. By applying magnetic perturbation as expected from [9], we reduce the slope to 0 or make it even slightly negative at q_{95} = 3.5. This shows that, indeed ELM deposition patterns are controlled by RMP. Interestingly we do see, that at q95 = 4.1 *A* becomes positive for P_{tot} = 6 MW and 9 MW and then again becomes 0 at q95 = 4.3.

Lowest graph in Figure 3 presents toroidal asymmetry between mean values of ELM energy detected at two different locations in given phase -$R = \langle E_{dep}^{FLIR} \rangle / \langle E_{dep}^{SBFP} \rangle$. With $\langle E_{dep} \rangle$ defined as a mean energy over inner and outer leg. As expected from previous works [3,11] without RMP this ratio oscillates around value of R = 1 independent on q95. Applying magnetic perturbation introduces asymmetries up to 20% between two toroidal locations. The value of *R* changes with safety factor, with amplitude stronger in the case of higher heating power. The asymmetry is most likely caused by the 3D structure of stochastic boundary, which is very sensitive to the safety factor profile. One of the effects of changing q_{95} is modification of the lobe position on a target [15], which is most likely the explanation of variation of toroidal asymmetry with safety factor during the RMP. Please note, that the asymmetries are stronger at higher heating power, which again suggests better coupling of perturbation fields with plasma equilibrium.

As seen above on DIII-D similar to other experiments on average power loads due to type-I ELMs are toroidally symmetric with variability of about 50%. This can be well understood if we compare dynamics of heat load patterns as measured by two cameras during an ELM. This is presented in Figure 4a, where heat flux density evolution is presented during the same event as measured by two cameras (left graph – SBFP, righ one – FLIR). Although we observe that rise time of power flux and decay are in the same order, evolution and structures are rather different at two toroidal locations. Applying 5 kA of I-coil current

creates stochastic boundary in the plasma edge and specific structure of manifolds intersecting the target plates. In the discharge #139743 with q95 = 3.5 this results with a small mitigated ELMs depositing on average to the divertor about 3 kJ. As can be seen in Figure 4b-c they all have very similar structure, which follows inter-ELM stochastic footprints. Smaller ELMs with $E_{dep} \leq 2$ kJ form two substructures on the target, whereas those with higher E_{dep} create a third lobe at about 70-80 mm from the separatrix. This is rather consistent with findings in [9]. They expel enough energy through a SOL in order to fill that outer lobe.

One of the important questions for ITER is in how far RMP can realize scenario with small ELMs, which do not exceed certain level of heat loads. It is assumed that the upper level of energy deposited during an ELM is 2% of energy stored in the plasma volume, which is rather low value if we consider results of present machines operating in H-mode scenarios [3]. In Figure 5 a probability distribution of ELMs with given energy is shown. The data is collected from all four investigated discharges and the probability distribution is calculated separately for different phases of the discharge.

1. In the initial phase (topmost graph), there is rather weak if any at all effect of perturbation fields on ELMs. All distributions for different values of q95 have rather similar shape with maximum between 2 and 4 kJ. In the case of q95 = 3.7, black curve, there is no ELMs larger then 7 kJ in contrary to other discharges.
2. A second graph presents data for the non-RMP phase of the discharge. Here we observe rather wide spectrum of ELMs with different energies with few cases of ELMs even with energy between 18 and 20 kJ. As expected those curves do not show any clear dependence on safety factor profile.
3. Applying RMP at t = 2200 ms clearly changes distribution of ELM energies by shifting ELM energies towards lower values below 2 kJ. The most optimal case is

reached at q95 = 3.5, where almost 90% of all events fall into energy range 0 – 2 kJ and few ELMs having energies of order of 4 -7 kJ. At higher q95 the amount of small ELMs is reduced. Please note, that distributions at q95 = 3.9 and 4.3 are rather similar, which was also true for values of R and *A* in Figure 3. This suggests that similar to effect of magnetic perturbation on plasma pressure profile [20] also mitigation of ELMs by RMP has more than one resonant window.

4. Increasing heating power to 9 MW as expected from results discussed above improves the mitigation effect. All distributions have most of the events located below 5 kJ. In the case of q95 = 3.9 we did not detected single ELM with energy above 5 kJ. Also here a case at q95 = 4.3 (green curve) seems to have stronger influence of RMP on ELMs than the one at q95 = 4.1 (red curve). In the latter one there are still some events with $E_{dep} > 8$ kJ. Please note, that both cases without RMP are very similar.

Summary

In the paper we have discussed scenarios of H-mode plasmas with RMP, where instead of suppressing them completely we mitigate. With proper value of safety factor we could reach a discharge, where all ELMs deposit on average about 5 kJ to the lower divertor. The probability distribution made on inner leg shows that about 90% of events deposit less than 3 kJ at the location of SBFP camera (i.e. at $\varphi = 135°$) and with no ELM depositing more than 5 kJ there. This is very promising for ITER as small, well controlled ELMs during the discharge help to exhaust impurities from the plasma volume and do not reduce lifetime and durability of divertor surface. The effects of RMP on ELM behavior seems to have few resonant windows with the optimum reached at $q_{95} \approx 3.9$ and $P_{tot} = 9$ MW. Worth noting is that at higher heating plasma response to magnetic perturbation is stronger, which is consistent with findings in [21].

Without RMP ELMs deposit on average the same energy on both investigated locations, however individual events show rather different structure and evolution of heat flux patterns. ELM wetted area on divertor surface increases linearly with an ELM energy. Value of the slope of the linear fit depends on q_{95}. Applying RMP forces ELMs to deposit power along channels defined by the manifolds of the stochastic boundary which introduces toroidal asymmetries, but significantly reduces ELM energies and their wetted area.

Bibliography

[1] F. Wagner, et al., Plasma Physics and Controlled Fusion 48 (2006) A217-A239.

[2] H. Zohm, Plasma Physics and Controlled Fusion 38 (1996) 105-128.

[3] A. Loarte, et al., Plasma Phys. Control. Fusion 45 (2003) 1549-1569.

[4] A. Kirk, et al., Plasma Physics and Controlled Fusion 47 (2005) 315-333.

[5] A. Herrmann, Journal of Nuclear Materials 363-365 (2007) 528-533.

[6] A. Kirk, et al., Phys. Rev. Lett. 96 (2006) 185001-4.

[7] M. W. Jakubowski, et al., Journal of Nuclear Materials 390-391 (2009) 781-784.

[8] T. Eich, A. Herrmann, J. Neuhauser, Phys. Rev. Lett. 91 (2003) 195003.

[9] M. W. Jakubowski, et al., Nuclear Fusion 49 (2009) 095013.

[10] G. Federici, et al., Nuclear Fusion 41 (2001) 1967-2137.

[11] A. Herrmann, Plasma Phys. Control. Fusion 44 (2002) 897-917.

[12] T. Evans, et al.,Journal of Nuclear Materials 390-391 (2009) 789-792.

[13] T.E. Evans, et al., Nat Phys 2 (2006) 419-423.

[14] T. Evans, et al., Nuclear Fusion 48 (2008) 024002.

[15] O. Schmitz, et al.,Plasma Physics and Controlled Fusion 50 (2008) 124029.

[16] T.E. Evans, R.A. Moyer, P. Monat, Phys. Plasmas 9 (2002) 4957-4967.

[17] A. Herrmann, et al.,Plasma Physics and Controlled Fusion 37 (1995) 17-29.

[18] T. Eich, et al., Plasma Physics and Controlled Fusion 49 (2007) 573-604.

[19] R. Fitzpatrick, Phys. Plasmas 10 (2003) 1782.

[20] O. Schmitz, et al., Phys. Rev. Lett. 103 (2009) 165005.

[21] D. Orlov, et al.,Nucl. Fusion 50 (2010) 034010.

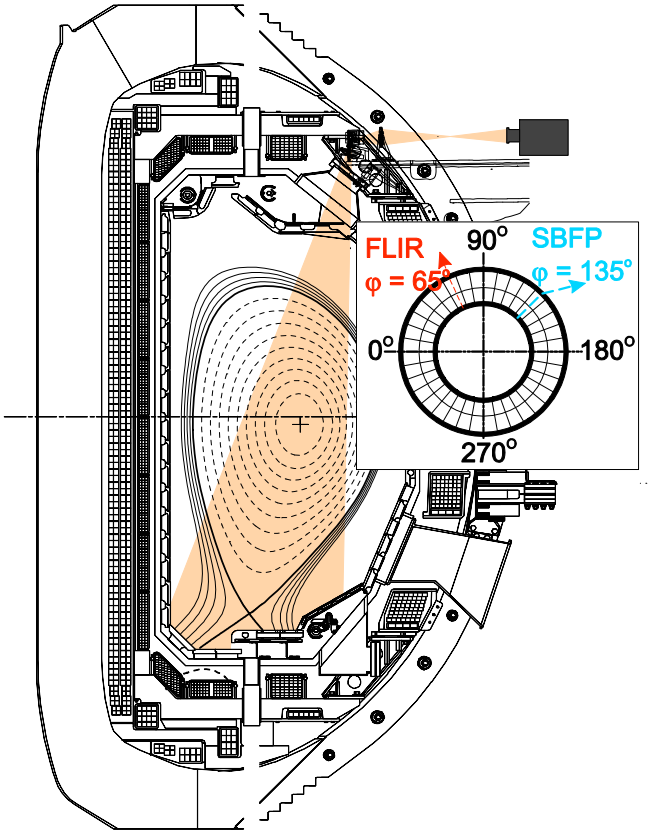

Figure 1. Sketch presenting set-up used to measure the heat flux by both cameras: FLIR located at 65 deg and SBFP at 135 deg (see inlay). Shape of plasma equilibrium was optimized for IR observation of both legs.

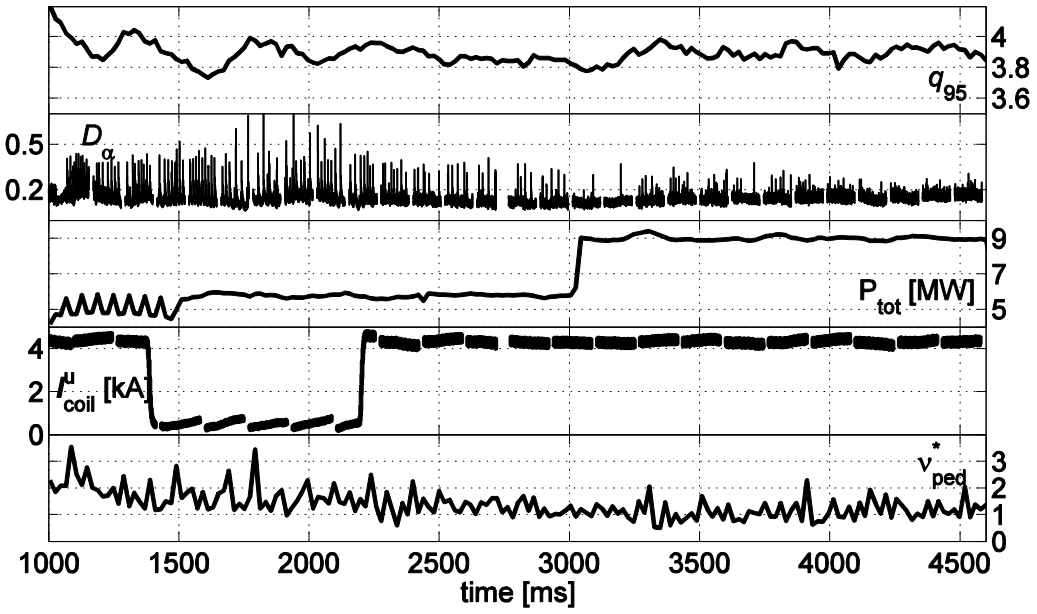

Figure 2. Overview of main plasma parameters for the discharge #139745 – from top: safety factor at ψ_{95} (q_{95}), total heating power (P_{tot}), current amplitude in RMP coils (Icoil) and electron pedestal collisionality.

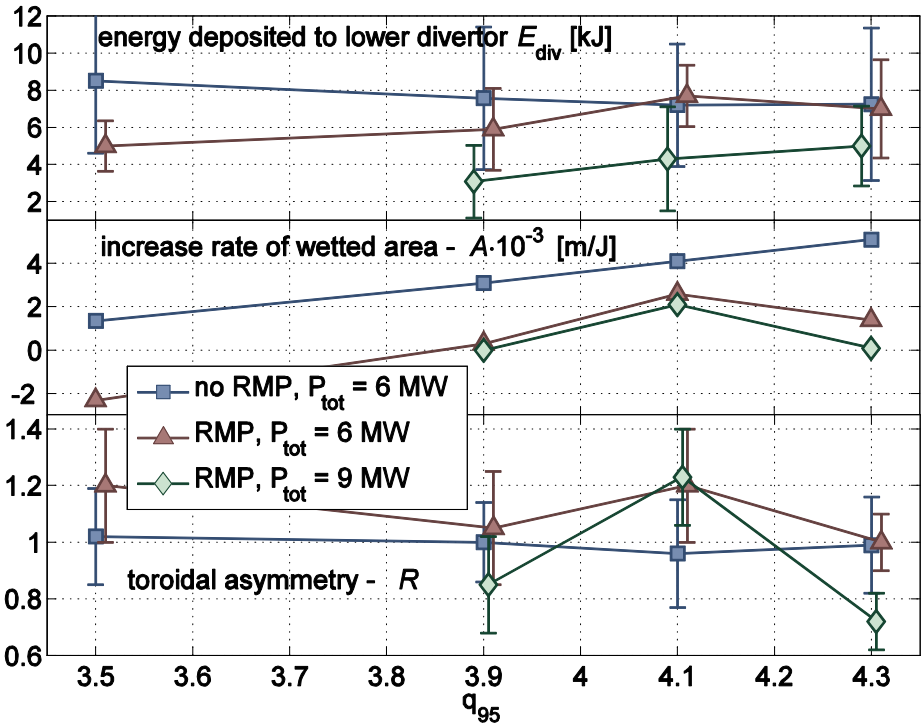

Figure 3. Dependence of several parameters characterizing heat loads to the lover divertor on q95 - from top: total energy deposited to the divertor (sum of inner and outer leg), increase rate of wetted area with ELM size, toroidal as

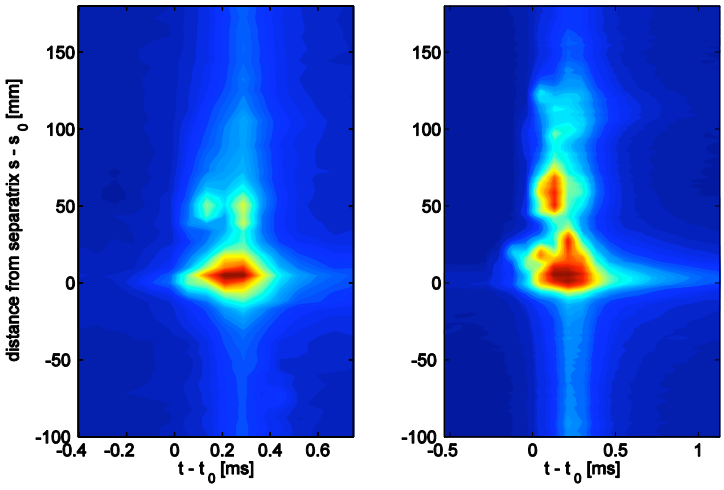

a)

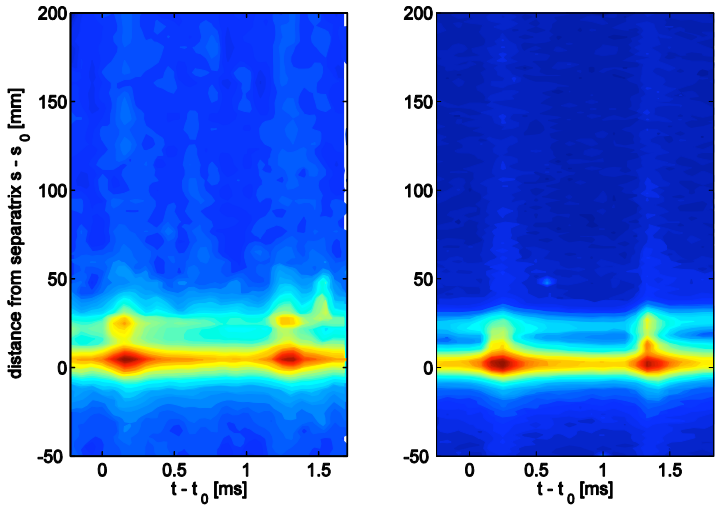

b)

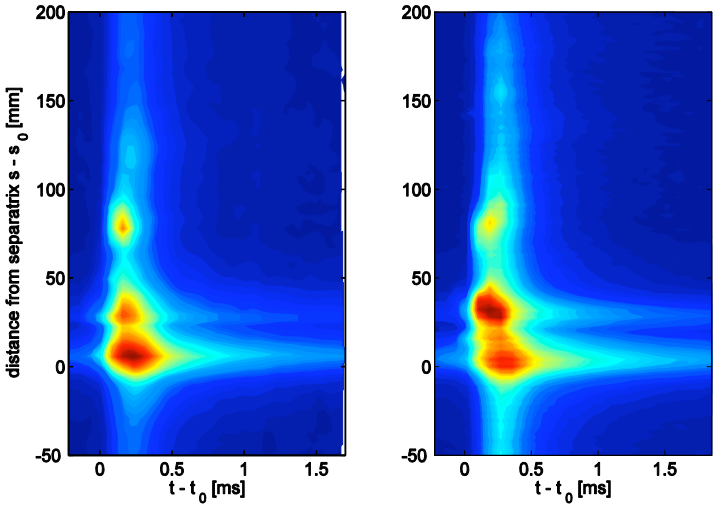

c)

Figure 4. An example of type-I ELM evolution on divertor surface measured by two different cameras (left SBFP at 135 degrees, right FLIR at 65 degrees) during no RMP phase (a) and with RMP applied - #139743, q95 = 3.5 (b-c).

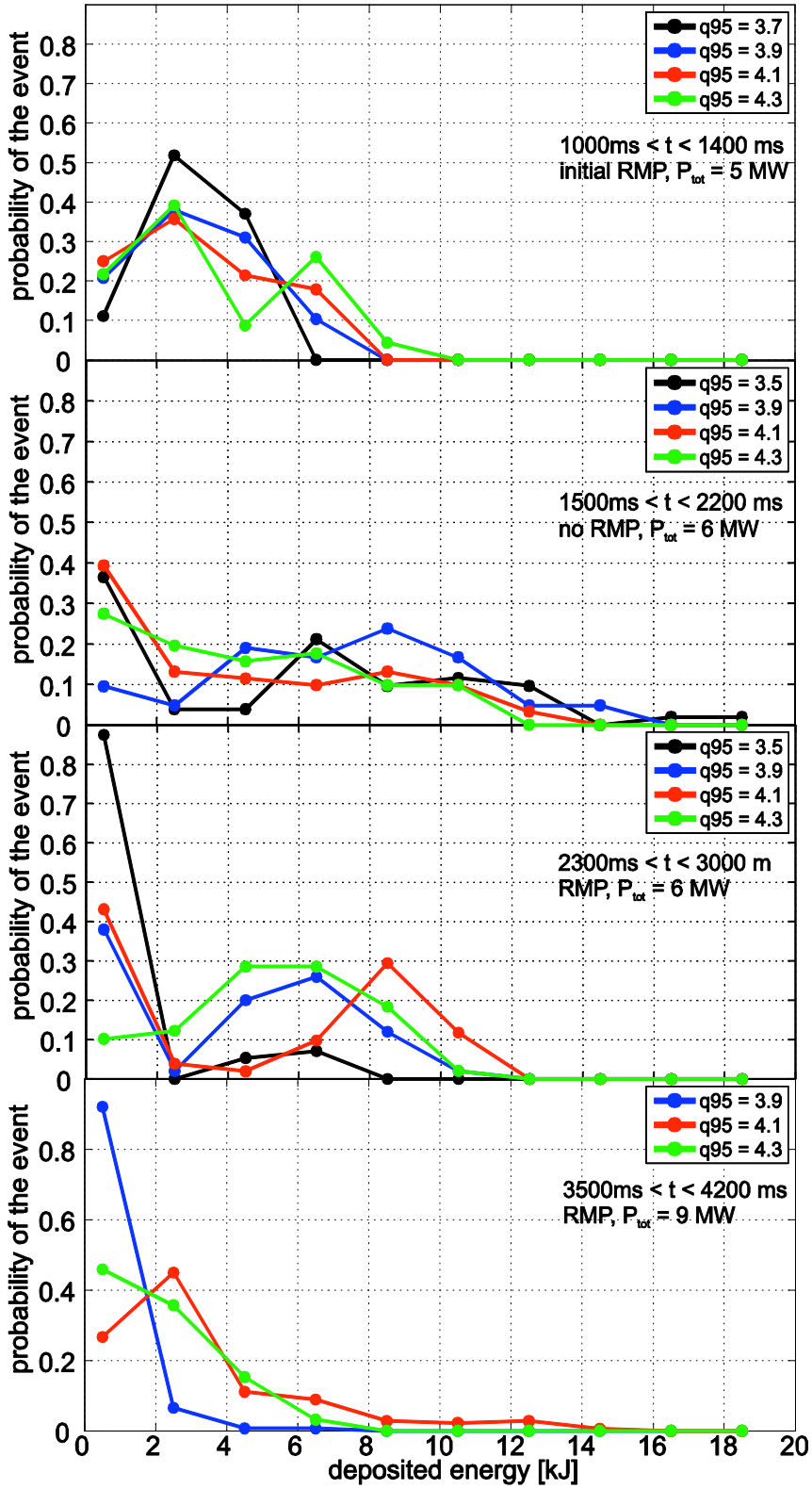

Figure 5. Probability distribution of ELM energies as measured bythe SBFP camera on inner divertor surface. Different colors of curves indicate different discharges (black – #139743, q95 = 3.5; blue - #139745, q95 = 3.9; red – #139747, q95 = 4.1, green - #139748).